Effects of thickness on the electrical properties of metalorganic chemical vapor deposited $Pb(Zr,Ti)O_3$ (25–100 nm) thin films on $LaNiO_3$ buffered Si

C. H. Lin, P. A. Friddle, C. H. Ma, A. Daga, and Haydn Chen[a)]
Department of Materials Science and Engineering, Frederick Seitz Materials Research Laboratory, University of Illinois at Urbana-Champaign, Urbana, Illinois 61801

(Received 5 September 2000; accepted for publication 3 May 2001)

$Pb(Zr, Ti)O_3$ (PZT) thin films with (100) preferred orientation were prepared using metalorganic chemical vapor deposition on $LaNiO_3$ (LNO) buffered platinized Si with thickness varying from 25–100 nm. The dependence of electrical properties of PZT films on thickness was studied using several techniques, including polarization–electric field ($P-E$), temperature variable current–voltage ($I-V$), and capacitance–voltage ($C-V$) measurements. Because of the formation of Schottky barriers at ferroelectric/electrode interfaces, built-in electric fields are present. A progressive increment in carrier concentration and interfacial built-in electric field versus reducing PZT film thickness was observed, which is believed to be a dominant factor controlling the measured dielectric/ferroelectric properties. The higher built-in electric field in thinner PZT films would pin the dipoles at the interfacial region and retard the response of dipoles to the external electric field. © *2001 American Institute of Physics.* [DOI: 10.1063/1.1383262]

I. INTRODUCTION

Recently, the fabrication of integrated ferroelectric nonvolatile dynamic random access memories (NV-DRAMs) has drawn much attention.[1] Several device structures have been proposed, such as the one transistor (1 T)/one capacitor (1C) structure used in conventional DRAM or the metal-ferroelectric-semiconductor field effect transistor (MFSFET).[2,3] One of the major concerns in the development of ferroelectric based NV-DRAMs is the scaling limit of ferroelectric switching, since this limitation would affect the size of the device fabricated. Currently, most studies of PZT thin films have been focused on the film thickness range of 100–300 nm. There are few reports concerning the ferroelectric properties of PZT films below 100 nm in thickness, which is an objective of the current investigation.

One of the most pronounced size effects in the PZT thin films is the drastic increase in coercive field (E_c) and decrease in remanent polarization (P_r) with the reduction in thickness. There have been several studies about this subject.[4–7] It was suggested that the thickness dependence of ferroelectric properties originates from either a disordered interfacial layer or a built-in interfacial potential.

Lakeman *et al.*[4] and Larson *et al.*,[5] adopted the concept of a series capacitor model. It was assumed that a low dielectric constant interfacial disordered layer is in series connection with the ferroelectric layer. Consequently, the actual electric field (E_f) across the ferroelectric layer is smaller than the applied electric field (E) because of the continuity condition of electric displacement (D) between the interfacial disordered layer and the ferroelectric layer. Later, Tagantsev *et al.*[6] proposed a built-in field assisted domain nucleation model. It was suggested that the nucleation of domains for polarization reversal was assisted by the interfacial built-in electric field (E_{bi}), which is induced by the metal/ferroelectric Schottky junction. In case the built-in electric field decreases with the film thickness, the coercive field would increase and remanent polarization would decrease with diminishing film thickness. The third model considered charge injection from the electrode into the near-electrode trap states in the ferroelectric layer as a dominant effect.[7] Charge exchange processes between the electrode and the near-electrode trap states during measuring cycles were described to modify the measured ferroelectric properties. As the film becomes sufficiently thinner, the near-electrode trap states occupy a larger portion of the ferroelectric layer; therefore, the coercive field shows a dependence on thickness.

However, on the basis of the $I-V$ and $C-V$ results in the current study, the variation of carrier concentration with film thickness in conjunction with the Schottky barrier formed at ferroelectric interface are suggested to have the dominant effect on the measured ferroelectric properties. The objectives of the present study are: (1) to identify the origin of change of hysteresis behavior with respect to thickness, especially for films thinner than 100 nm, and (2) to correlate the switching behavior with the interfacial structure, especially the effects of space charge, using temperature dependent $C-V$ and $I-V$ techniques.

II. EXPERIMENT

LNO (0.2 μm) thin films with (100) preferred orientation were deposited on $Pt(0.15\,\mu m)/Ti(0.05\,\mu m)/SiO_2(0.15\,\mu m)/Si$ substrates by radio frequency (rf) magnetron sputtering at 300 °C. Before PZT deposition, the LNO-covered substrates were annealed at 800 °C for 30 min. This

a)Author to whom correspondence should be addressed; electronic mail: h-chen2@uiuc.edu

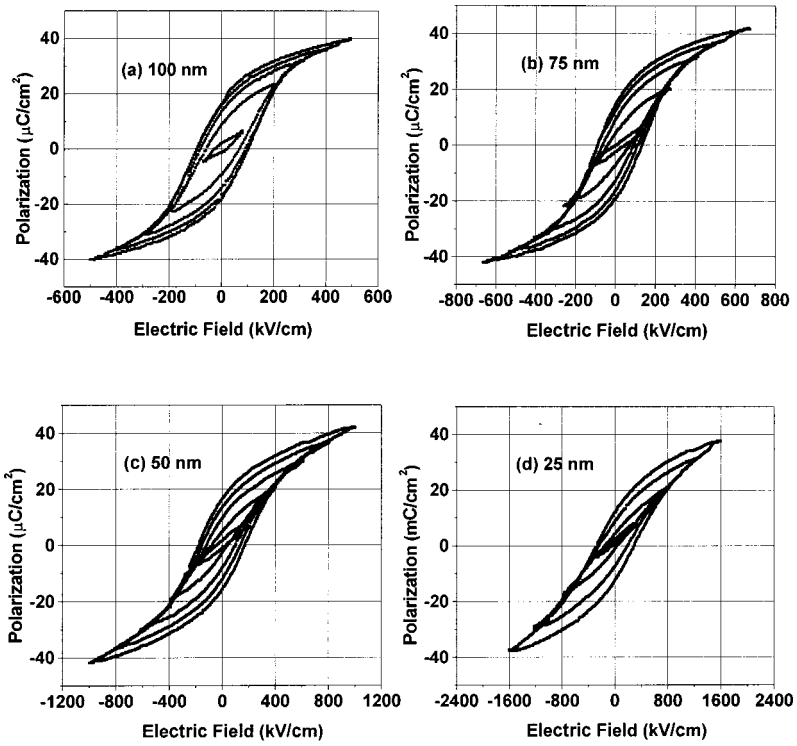

FIG. 1. $P-E$ characteristics of PZT thin films with different thickness under 1–5 V.

heat treatment was found to be a critical process for obtaining PZT thin films with optimal properties. Although it was reported[8] that a LNO layer could be fully crystallized at 350 °C with a prolonged anneal of about 120 min, such an annealing process did not allow for the deposition of high quality PZT layers.[9] For LNO films deposited at lower temperature (250–350 °C), they already showed (001) oriented fibrous grains with lateral grain size typically below 500 Å. It was also observed that a certain amount of amorphous phase existed at grain boundaries.[9] With an annealing process at 800 °C, the grains became columnar in shape with lateral grain size ranging from 500–1000 Å. PZT layers grow on LNO via a grain-to-grain epitaxial relationship. Consequently, if the LNO layer has small grain size or a nonuniform distribution of grain sizes, the grown PZT layer will have a similar microstructure, thereby degrading the ferroelectric properties. It was found in our study that the LNO layers have to be annealed at temperatures as high as 700–800 °C to obtain satisfactory quality. The subsequent PZT thin film growth was then carried out in a low pressure, horizontal and cold-wall quartz reactor with a resistive substrate heater at 600 °C. The metalorganic sources used were $Pb(TMHD)_2$, $Zr(OC_4H_9)_4$, and $Ti(OC_3H_7)_4$. The vapor delivery used ultrahigh purity nitrogen as the carrier gas.

X-ray diffraction (XRD) scans were carried out using a Philips diffractometer with Cu $K\alpha$ radiation to determine the phase(s) present and the crystalline orientation of PZT layers. A Philips CM-12 transmission electron microscope (TEM) was used to measure the film thickness in cross-sectional view. For electrical property measurements, Au (2000 Å thick) square patterns ($200\,\mu\text{m}\times 200\,\mu\text{m}$) were evaporated onto PZT thin films as the top metal electrodes of the metal-ferroelectric-metal (MFM) structure. A Sawyer–Tower circuit was employed for measuring the hysteresis behavior ($P-E$ loop). The $C-V$ behavior was measured by employing an HP 4276 LCR (inductance–capacitance–impedance) meter with an external dc source. A Keithley 236 source measurement unit was used to measure $I-V$ characteristics. The dc voltage-sweeping rate for both $C-V$ and $I-V$ measurements was 0.01 V/s.

III. RESULTS AND DISCUSSION

A. Hysteresis behavior

The $P-E$ curves of 25–100-nm-thick PZT thin films with applied voltage ranging from 1 to 5 V are shown in Fig. 1. It was found that the P_r values of 50–100-nm-thick films are all in the range of 17–20 μC/cm^2 for an applied voltage of 5 V. Also, the coercive voltages (V_c) are all within 0.8 to 1 V. However, the 25 nm thick films broke down at 5 V. For 4 V applied voltage, the P_r value of the 25 nm thick film is around 10 μC/cm^2 with the V_c value being 0.6 V.[10] The P_r values obtained in the present study are lower than those recently reported by Wouters *et al.*,[11] where it was reported that the P_r value of sol-gel derived ⟨111⟩ oriented 75-nm-thick PZT thin films on Pt/Si is around 30 μC/cm^2 with a 2 V applied voltage. However, our P_r values are comparable with those of PZT films grown on other perovskite oxide electrodes.[7,12] The ⟨001⟩-oriented 60-nm-thick PZT thin films epitaxially grown on YBCO/$LaAlO_3$ by Bjormander *et al.*[12] have similar P_r values ($\cong 20\,\mu$C/cm^2) to those reported here. Moreover, the P_r values of 100–600-nm-thick ⟨001⟩-oriented PZT deposited on LSCO/Si, as reported by Cillessen *et al.*,[7] are around 20 μC/cm^2. Thus, the lower P_r values in this study compared with the P_r reported by Wouters *et al.*[11] might be due to difference in the film orientation. It is known that ⟨111⟩-oriented sol-gel derived PZT films on Pt or RuO_2 layers generally show higher P_r values than

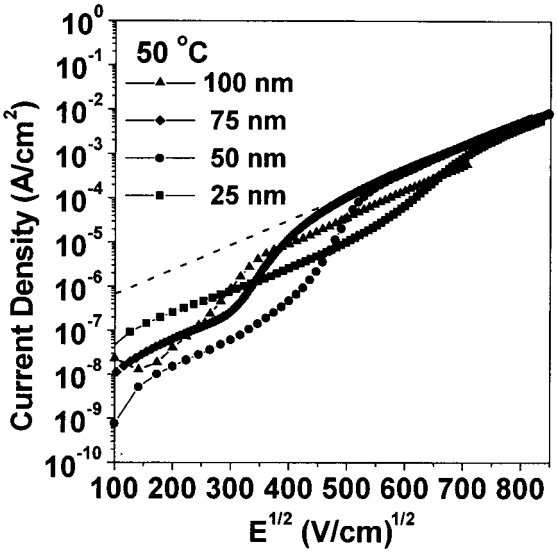

FIG. 2. Current density (J) vs ($E^{1/2}$) plots of PZT thin films.

⟨001⟩-oriented PZT films. It is suggested that using an electric field to reorient the permanent dipole moment along the ⟨111⟩ direction is easier than ⟨001⟩ direction due to the multiplicity.[11,13]

The most important observations of the ferroelectric properties resulting from a reduction of film thickness are: (1) an appreciable increase of the coercive field and (2) a noticeable decrease of the remanent polarization under the same applied field. We shall propose a model to explain these observations. The model suggests that the built-in potential, caused by the space charge inside the film, impedes the polarization switching and raises the coercive field. This mechanism will be discussed in Sec. III D with the support of $I-V$ and $C-V$ results.

B. Current–voltage ($I-V$) behavior

The $I-V$ characteristics of PZT films are shown in Fig. 2 in the form of a $\ln(J)$ vs $E^{1/2}$ plot. Data were collected at 50 °C to reduce the noise caused by moisture. Positive voltage was applied to the bottom (LNO) electrode and increased stepwise (0.01V/s). Several mechanisms have been proposed to describe the $I-V$ characteristics of PZT thin-film capacitors. Sudhama *et al.*[14] proposed a two-carrier thermionic emission model, whereas a space charge layer-influenced Schottky-emission mechanism was described by Stolichnov *et al.*[15] and Wouters *et al.*[16] Zhang *et al.*[17] also proposed a back-to-back Schottky emission model, which was similar to the Stolichnov's model but the band bending inside PZT layer was defined differently.

In the studies of Stolichnov *et al.* and Wouters *et al.*,[15,16] an upward band bending with hole injection at the interfaces was suggested. However, downward band bending with electron injection at the interfaces was suggested by Scott[18] and Zhang *et al.*[17] The differences in band bending and injected charge result from different electron affinity values of PZT employed in those studies. The electron affinity (χ_e) value used in the studies of Stolichnov *et al.* and Wouters *et al.* was 2.6 eV, which was determined from electron emission.[19] Scott determined the value of electron affinity (χ_e) to be 3.4 eV using x-ray photoelectron spectroscopy (XPS).[18]

Most proposed mechanisms for the $I-V$ behavior are similar to the metal-semiconductor-metal (MSM) diode model derived by Sze.[20] For convenience, our description follows an illustration that is similar to the space charge layer influenced Schottky emission mechanism proposed by Stolichnov.[15] They suggested that a hole accumulation layer forms at the interface between the PZT film and the electrode, and an upward band-bending forms inside the PZT. Under a sufficiently large applied voltage, the depleted space charge layers from the bottom and the top electrodes touch each other. This voltage is denoted as the reachthrough voltage. As the voltage is further increased, a flat-band condition is achieved. At the flat-band condition, the film becomes fully depleted and Schottky emission becomes the dominant mechanism controlling the $I-V$ characteristics. If a downward band bending forms inside PZT, electronic inversion layers at the interfaces is suggested.[17,18]

There are two important conditions in the proposed mechanism: (1) flat-band voltage (V_{fb}), and (2) Schottky emission. The flat-band voltage (V_{fb}), which corresponds to the potential required to deplete the interfacial space charge, of a metal-semiconductor-metal (MSM) diode was shown to be[20]

$$E_{fb}=\frac{V_{fb}}{W}=\frac{qNW}{2\varepsilon_0\varepsilon_s}, \tag{1}$$

where W is the film thickness, ε_0 is the vacuum permittivity, ε_s is the dielectric constant of the material, q is the electronic charge, and N is the carrier concentration. For Schottky emission, the reverse saturation current (J) due to image force lowering can be written as[20]

$$J=A^*T^2\exp\left(\frac{-q[\phi_b-(qE/4\pi\varepsilon_0\varepsilon_r)^{1/2}]}{k_BT}\right), \tag{2}$$

in which A^* is the Richardson constant, Φ_b is the barrier height for charge injection, E is the external field strength, T is the measuring temperature, and k_B is the Boltzmann constant. The term $(qE/4\pi\varepsilon_0\varepsilon_r)^{1/2}$ represents the effect of image force lowering.

Figure 2 shows that the $\ln(J)$ vs $E^{1/2}$ plots approach a linear region with the same slope for all film thickness, as indicated by the dashed line. In the MSM diode model, the specific electric field corresponding to the onset of the linear region in the $\ln(J)$ vs $E^{1/2}$ plot is the flat-band voltage (V_{fb}) at which the Schottky emission is initialized. Before the Schottky emission process is initialized, the conduction mechanism is a thermionic emission process in which the carrier must overcome a potential barrier ($\Delta\phi$) caused by band bending, where $\Delta\phi$ defines the extent of band bending in PZT. Since the value of $\Delta\phi$ changes with the applied voltage, the $\ln(J)$ vs $E^{1/2}$ plots show a nonlinear region until the flat-band voltage is attained.[14,15,17]

We converted the flat-band voltage to the corresponding electric field across the film, which is denoted as flat-band electric field (E_{fb}). From Fig. 2, the flat-band electric fields for PZT were found to increase with decreasing thickness.

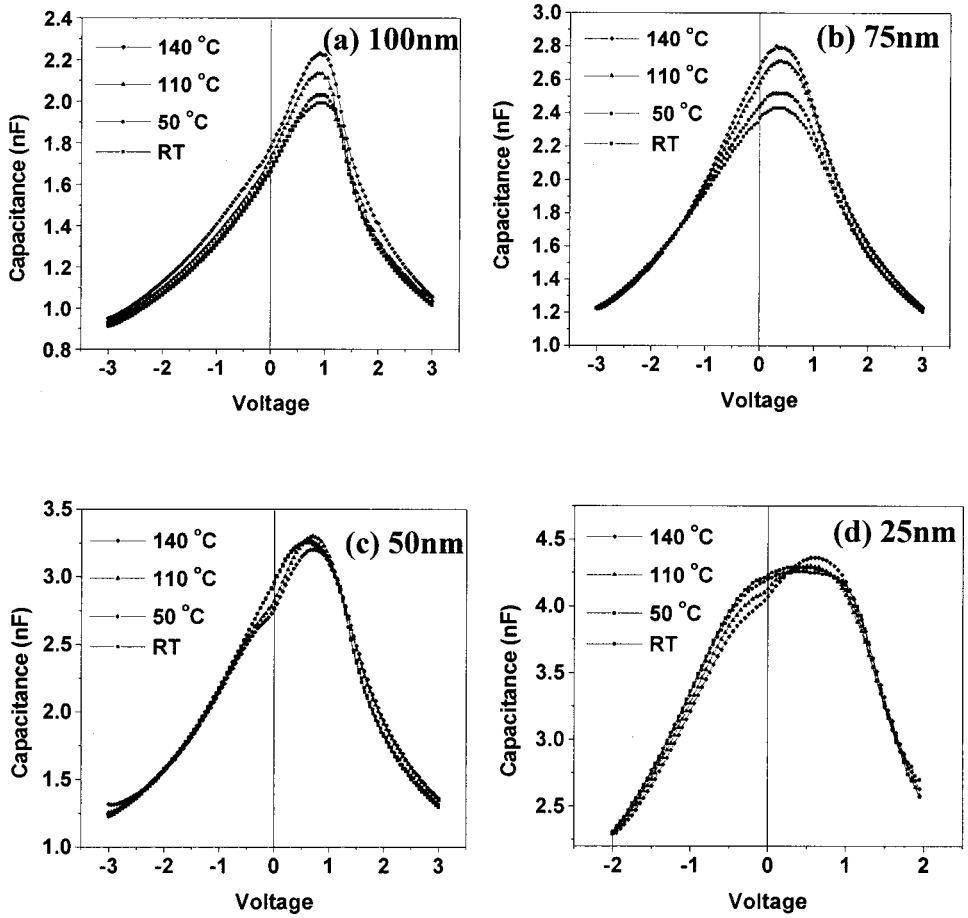

FIG. 3. Temperature dependent $C-V$ behavior of (a) 100, (b) 75, (c) 50, and (d) 25 nm PZT thin films.

The flat-band electric fields were determined to be 640, 300, and 120 kV/cm for 25, 50, and 100 nm thick films, respectively, (75 kV/cm for 200 nm films[9] with same process condition). It can be seen from Eq. (1) that E_{fb} is a function of N and W. Therefore, the $I-V$ results indicate that the thinner PZT films have higher carrier concentration (N). Using the experimentally measured flat-band voltage, carrier concentrations of 100, 50, and 25 nm thick PZT were calculated to be, 7×10^{18}, 3.15×10^{19}, and $1.3\times10^{20}\,\mathrm{cm}^{-3}$, respectively, ($1.9\times10^{18}\,\mathrm{cm}^{-3}$ for 200 nm films with same process condition). As a comparison, the carrier concentration obtained in Stolichnov's study is $5\times10^{17}\,\mathrm{cm}^{-3}$ for a 300 nm thick PZT.[14] For perovskite PZT, the atomic concentrations of Pb and oxygen are 1.56×10^{22} and $4.62\times10^{22}\,\mathrm{cm}^{-3}$, respectively. Considering the final constituents of the film to be slightly deviated from the exact stoichiometry due to thermal processing cycles, then Pb or oxygen vacancies could form which would create two holes or electrons, respectively. If only one type of defect (for example, Pb vacancies) were present in PZT, the estimated vacancy concentrations, using the carrier concentration values obtained previously, are around 0.4, 0.1, and 0.02 at. % for 25, 50, and 100 nm thick PZT, respectively. It is reasonable for thinner PZT films to have more vacancy defects because of the high temperature processing in film growth and electrode preparation, which could cause more atomic loss from thinner films.

C. Capacitance–voltage ($C-V$) behavior

In Fig. 3, the temperature-dependent $C-V$ characteristics, with voltage sweeping from negative to positive values (upward sweeping), of 25-100-nm thick PZT thin films are illustrated. For films thicker than 75 nm, the capacitance values gradually increase with increasing temperature, because the dielectric constant of PZT increases with temperature ($T<T_c$). In addition, all curves have their peak values located at around 0.5–1 V, which corresponds to the coercive voltages for an upward voltage sweep. As the film thickness is reduced to 50 nm, the capacitance values do not increase appreciably with increasing temperature. Moreover, a shoulder next to the peak is found near zero voltage, which becomes more noticeable with increasing temperature (50–140 °C). For the $C-V$ curves of 25-nm-thick PZT films, the peak in capacitance occurs at 0.8 V and a shoulder near zero voltage appears at all measuring temperatures (20–140 °C). Similar behavior should be observable while the voltage is sweeping downward from positive to negative value, only the shoulder would show up on the positive voltage side (near 0 V).[10]

The $C-V$ behavior of PZT thin films have been discussed by Chai *et al.*,[21] in which they showed that two factors control the $C-V$ behavior: (1) domain switching, and (2) distribution of space charge in the film. The variation of capacitance for a ferroelectric material is traditionally con-

sidered to be due to domain switching from one poling state to the other when the dc voltage is swept from, for example, negative to positive. For very thin films (25–50 nm), the variation of space charge distribution and therefore the built-in electric field near the PZT/electrode interface becomes more significant than thicker films. The $C-V$ results indicate that the space charge variation becomes a dominant factor and the polarization behavior is greatly affected by the electric field distribution in these PZT thin films. The shoulder at $V=0$ and the invariance of measured dielectric constant with temperature indicate a space charge effect. Following the metal-semiconductor-metal diode model[20] (described in Sec. III B) illustrating the $I-V$ behavior, it was suggested that the space charge in the PZT film gradually varies from hole-accumulation or electron inversion at the PZT/electrode interface to a full-depletion status under the applied dc voltage.

The $C-V$ behavior of those thinner PZT films (thickness $\leqslant 50$ nm) can be understood from semiconductor physics. It is known that the depletion layer width (W_d) and junction capacitance (C_j) of a semiconductor/metal junction can be expressed as[20]

$$W_d=\left(\frac{2\varepsilon_r\varepsilon_0(V_0+V)}{qN}\right)^{1/2}, \tag{3a}$$

and

$$C_j=A\left(\frac{q\varepsilon_r\varepsilon_0}{2(V_0+V)}N\right)^{1/2}, \tag{3b}$$

where V is the reversed bias voltage, V_0 is the built-in potential, N is the carrier concentration, and ε_r is the dielectric constant of the material.

Equations (3a) and (3b) show the variation of depletion width (W_d) and junction capacitance (C_j) with the applied voltage. While applying a negative dc voltage at the bottom electrode, the space charges become less populated (or more depleted) near the PZT/electrode interface, and this reduces the overall measured capacitance [i.e., Eq. (3b)]. As the voltage increases to about zero, the space charges become more populated (or less depleted) near both the top and bottom electrodes, thus the junction capacitance reaching a saturated value. Therefore, a shoulder located near zero voltage is observed. As the voltage further increases to positive values, the maximum capacitance value should occur at the coercive voltage (i.e., $\cong 0.5-1$ V for upward voltage sweep) because of polarization switching.

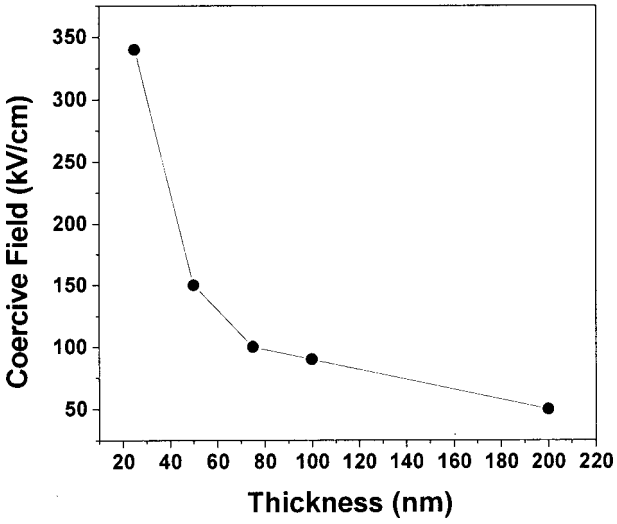

FIG. 4. Dependence of coercive field on the film thickness.

D. Effect of thickness on apparent ferroelectric properties: A space charge dominated effect

Figure 4 illustrates the dependence of coercive field (E_c) on the film thickness measured using 4 V applied voltage. As in the previous reports,[4–7] E_c values showed strong thickness dependence. It was reported by Chai *et al.*[22] that dipoles near the PZT/electrode interface are very difficult to switch if the carrier concentration exceeds $5\times10^{17}\,\mathrm{cm}^{-3}$, because these dipoles are pinned by the strong interfacial built-in electric field. Similar dipole pinning effects at interfaces were reported by Lee *et al.*[23] and by Sadashivan *et al.*[24] According to the relationship between the electronic band bending and electric field (E) [i.e., $E=(1/q)(\partial\phi_i/\partial x)$; where ϕ_i is the intrinsic Fermi level and q is the electronic charge], the electric field within PZT increases with the extent of band bend-

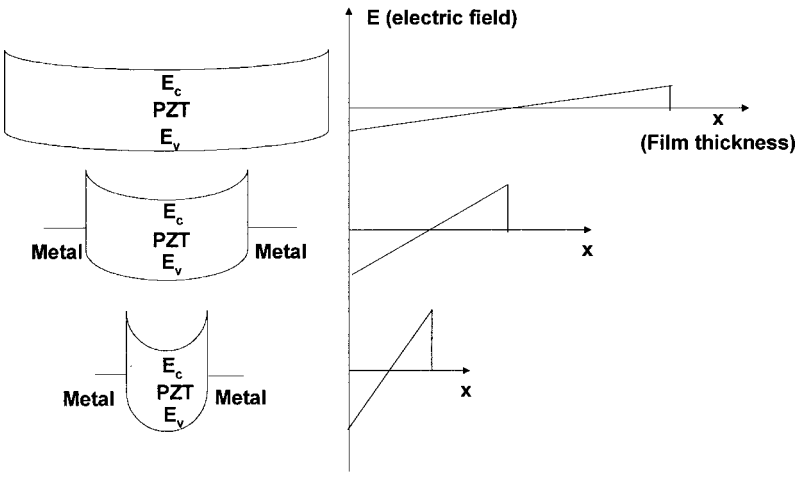

FIG. 5. Variation of band bending and electric field distribution inside PZT with respect to film thickness. The extent of band bending is larger for thinner films due to higher carrier concentration.

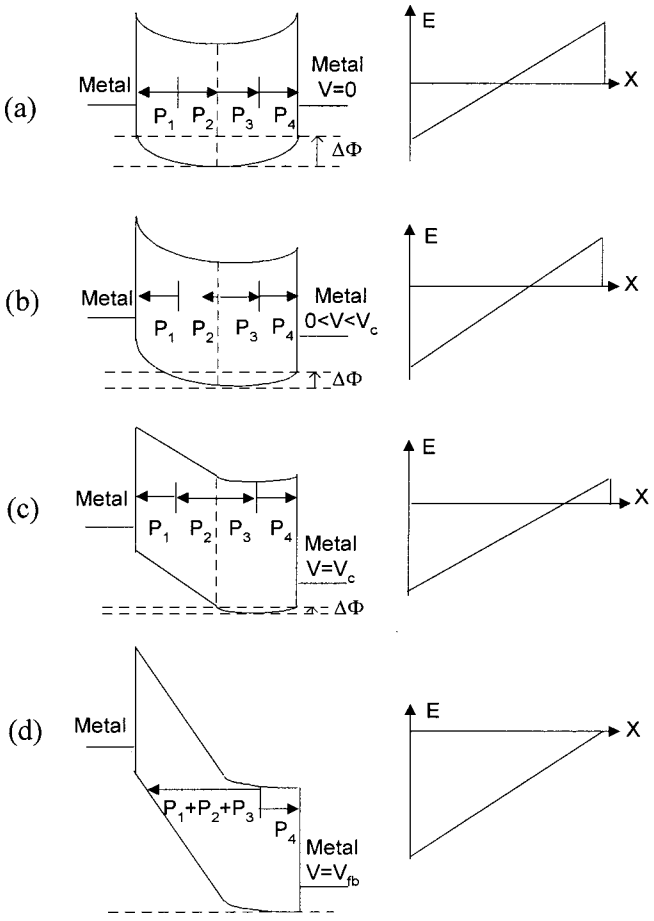

FIG. 6. The schematic of the effect of space charge on polarization switching. (a) At $V=0$, $(P_2+P_3+P_4-P_1)$ is the remanent polarization; (b) at $0<V<V_c$, P_2 is switched but value of P_2 is smaller than P_3; (c) at $V=V_c$, the total polarization is zero; (d) at $V>V_c$, P_3 is also switched. Also plotted is the corresponding variation of electric field (E) inside PZT with respect to applied voltage.

ing and gradually becomes stronger at interfaces, as illustrated in Fig. 5. In the interfacial space charge region, the dipoles have to comply with the interfacial built-in electric field and the dipoles are oriented in the same direction as the interfacial built-in electric field. As in Fig. 5, irrespective of upward or downward band bending at the interface, there exists a built-in electric field pointing toward the electrode at both interfacial regions that impedes the polarization switching because of the symmetrical nature of the MFM capacitor.

On the basis of our observations, we use a space charge dominated effect to describe the polarization behavior of PZT, as shown in Fig. 6, in which the case of upward band bending at the interfaces is illustrated. Microscopically, the process of dipole switching is affected by the band bending and electric field distribution within the film. A potential barrier ($\Delta\phi$) can be used to account for the magnitude of band bending within the film, as depicted in Fig. 6. The coercive field/voltage can be thought as the voltage that is required to overcome the potential barrier $\Delta\phi$ (band bending) and to deplete space charges within the film. The polarization switching process can be schematically described as follows. Figure 6 shows the film is partitioned into four parts with values of polarization P_1, P_2, P_3, and P_4 in each section, respectively (assuming that $P_1=P_2=P_3=P_4$ in magnitude in the beginning). It is assumed that P_1 and P_4 do not contribute much to the ferroelectric switching processes because they are pinned by the strong interfacial built-in potential. At $V=0$, the remanent polarization of the previous cycle is represented by $(P_2+P_3+P_4-P_1)$, as in Fig. 6(a). As the applied voltage (V) increases to $0<V<V_c$, the electronic band starts to tilt downward at the right-hand side and P_2 is switched to the other direction in response to the applied voltage, as in Fig. 6(b). The value of P_2 is still smaller than P_3, and P_1, P_3 and P_4 remain at approximately their original directions and values. As the applied voltage reaches the coercive voltage ($V=V_c$), it is strong enough to create band tilting and the electric field for P_2 to increase, as in Fig. 6(c). The magnitude of P_2 should be equal to P_3, since the measured macroscopic polarization (P) is 0 at $V=V_c$. As the applied voltage further increases to $V>V_c$, P_3 is also switched to the other direction [Fig. 6(d)].

The variation of measured coercive field (E_c) with film thickness, seen in Fig. 4, can also be rationalized through this space charge dominated effect. From the $I-V$ studies in Sec. III B it was found that the carrier concentration (N) increased with the reduction of film thickness. According to the Poisson equation (i.e., $\partial^2\Phi/\partial x^2=-\partial E_{bi}/\partial x=Nq$), the extent of band bending and the interfacial built-in potential increase with the carrier concentration (N). Therefore, thinner films have greater band bending and higher potential barrier, as illustrated in Fig. 5, for polarization switching because of their higher carrier concentration (N). The increase of measured coercive field with the reduction of film thickness can be explained by the increase of the carrier concentration (N) and the switching potential barrier ($\Delta\phi$). Other mechanisms can also contribute to the variation of coercive field with thickness.[4–7] However, our experimental results suggest that the space charge is one of the dominant mechanisms for determining the coercive field, especially for films thinner than 100 nm.

IV. CONCLUSIONS

PZT thin films with thickness ranging from 25 to 100 nm were deposited, using a metalorganic chemical vapor deposition technique, on the $LaNiO_3$ buffered platinized Si. The dielectric and ferroelectric properties showed strong thickness dependence in all of the following measurements: polarization–electric field ($P-E$), current–voltage ($I-V$), and capacitance–voltage ($C-V$). It was found that one of the root causes for the variation of electrical properties with thickness lies in the increase in carrier concentration with film thickness. $I-V$ results provided evidence for the increasing trend in carrier concentration with decreasing thickness. $C-V$ measurements show the modification of dielectric behavior due to space charge. On the basis of $P-E$, $I-V$, and $C-V$ measurements, the responses of built-in electric field and dipoles inside the PZT films were derived to illustrate the variation of ferroelectric properties with respect to thickness. Finally, it is suggested that effective control of

carrier concentration in the PZT films can be the major issue for resolving the influence of film thickness on the measured electrical properties.

ACKNOWLEDGMENTS

This work was supported by the U.S. Department of Energy under Grant No. DEFG02-96ER45439 through the Frederick Seitz Materials Research Laboratory at the University of Illinois at Urbana-Champaign. We acknowledge Dr. H. C. Kuo and S. W. Lee for their help in electrical measurements, and Professor T. B. Wu (National Tsing Hua University, Taiwan) for preparation of $LaNiO_3$ layers. A fruitful discussion with Professor David A. Payne was deeply appreciated.

[1] J. F. Scott and C. A. P. de Araujo, Science **246**, 1400 (1989).
[2] T. Yamazaki, K. Inoue, H. Miyazawa, M. Nakamura, N. Sashida, R. Satomi, A. Kerry, Y. Katoh, H. Noshiro, K. Takai, R. Shinohara, C. Ohno, T. Nakajima, Y. Furumura, and S. Kawamura, IEEE IEDM Tech. Dig. 613 (1997).
[3] S. Mathews, R. Ramesh, T. Venkatesan, and J. Benedetto, Science **276**, 238 (1996).
[4] C. D. Lakeman and D. Payne, Ferroelectrics **152**, 145 (1994).
[5] P. K. Larsen, G. J. M. Dormans, D. J. Taylor, and P. J. van Veldhoven, J. Appl. Phys. **76**, 2405 (1994).
[6] A. K. Tagantsev, Ferroelectrics **184**, 79 (1996).
[7] J. F. M. Cillessen, M. W. J. Prins, and R. M. Wolf, J. Appl. Phys. **81**, 2777 (1997).
[8] H. Y. Lee and T. B. Wu, J. Mater. Res. **13**, 2291 (1998).
[9] C. H. Lin, Ph. D thesis, University of Illinois at Urbana-Champaign, 2000.
[10] C. H. Lin, P. A. Friddle, X. Lu, H. Chen, Y. Kim, and T. B. Wu, J. Appl. Phys. **88**, 2157 (2000).
[11] D. J. Wouters, G. J. Norga, and H. E. Maes, Mater. Res. Soc. Symp. Proc. **541**, 381 (1999).
[12] C. Bjormander, K. Sreenivas, M. Duan, A. M. Grishin, and K. V. Rao, Appl. Phys. Lett. **66**, 2493 (1995).
[13] K. Aoki, Y. Fukuda, K. Numata, and A. Nishimura, Jpn. J. Appl. Phys., Part 2 **34**, 746 (1995).
[14] C. Sudhama, A. C. Campbell, P. D. Maniar, R. E. Jones, R. Moazzami, C. J. Mogab, and J. C. Lee, J. Appl. Phys. **75**, 1041 (1994).
[15] I. Stolichnov and A. Tagantsev, J. Appl. Phys. **84**, 3216 (1998).
[16] D. J. Wouters, G. J. Willems, and H. Maes, Microelectron. Eng. **29**, 249 (1995).
[17] L. Zhang, C. Lin, and T. P. Ma, J. Phys. D **29**, 457 (1996).
[18] J. F. Scott, Jpn. J. Appl. Phys., Part 1 **38**, 2272 (1999).
[19] A. V. Dixit, N. R. Rajopadhye, and S. V. Bhoraskar, J. Mater. Sci. **21**, 2798 (1986).
[20] S. M. Sze, *Physics of Semiconductor Devices* (Wiley, New York, 1981).
[21] F. K. Chai, J. R. Brews, R. D. Schrimpf, and D. P. Birnie III, J. Appl. Phys. **82**, 2517 (1997).
[22] F. K. Chai, J. R. Brews, R. D. Schrimpf, and D. P. Birnie III, J. Appl. Phys. **78**, 4766 (1995).
[23] J. J. Lee, C. L. Thio, and S. B. Desu, J. Appl. Phys. **78**, 5073 (1995).
[24] S. Sadashivan, S. Aggarwal, T. K. Song, R. Ramesh, J. T. Evans, Jr., B. A. Tuttle, W. L. Warren, and D. Dimos, J. Appl. Phys. **83**, 2165 (1995).